RESPONSE OF SQUEEZE-CAST Mg-Y-Nd-Sc-Mn ALLOY TO ANNEALING WITH CONSTANT HEATING RATES

Veronika KODETOVÁ, Martin VLACH, Ivana STULÍKOVÁ, Bohumil SMOLA, Bohumil HORNÁT, Tomáš KEKULE

Charles University in Prague, Faculty of Mathematics and Physics, Prague, Czech Republic, EU, veronika.kodetova@seznam.cz

Abstract

The MgYNdScMn alloy was squeeze-cast under a protective atmosphere. Precipitation reactions were studied by differential scanning calorimetry. Additionally the electrical resistometry and hardness measurements were performed. Transmission electron microscopy of specimens quenched from temperatures of significant thermal changes were used to identify microstructural processes responsible for these changes. The measurements revealed three exothermic effects connected to complex precipitation processes. No direct evidence was observed for the first effect. As this early stage is associated with small resistivity and hardness changes, we suppose a submicroscopic formation of a transient *β''* phase there. Precipitation of the transient *β'* phase in the form of fine plates was observed at 270 °C. A weak thermal reaction corresponding to this process was detected only for heating rates of 1 and 5 K/min. The *β'* phase subsequently transforms into the stable *β* phase. Discs of the Mn_2Sc phase parallel to basal planes and thin basal Mn-rare earth plates of a transient hexagonal phase were observed simultaneously after annealing up to 390 °C. The main resistivity decrease in the range 270 - 390 °C is caused by precipitation of these three phases. The apparent activation energy for the early stage, $Q = (119 \pm 10)$ kJ·mol^{-1}, and for *β* phase, $Q = (147 \pm 10)$ kJ/mol, corresponds excellently to the results obtained in our previous study in ternary MgYNd and WE43 alloys, respectively.

Keywords: DSC, hardness, electrical resistivity, phase transformation, electron microscopy

1. INTRODUCTION

High thermal stability of precipitated phases in Mg-based alloys is decisive for a reasonable stability of mechanical properties. A number of cast Mg alloys containing rare earth elements (RE) have been investigated recently, e. g. Refs. [1-3]. These investigations have shown that RE and similar elements Y and Sc can be used to adjust mechanical properties with a wide range of alloy compositions and heat treatments [4, 5]. Two basic sequences of the supersaturated solid solution decomposition are known in binary Mg-RE alloys: Mg-Gd type and Mg-Ce type [4, 6, 7]. These decomposition sequences can be modified in Mg alloys with combination of RE from different groups and in complex alloys with the addition of further elements [8]. Modification of precipitation sequences and phase morphology in Mg-RE base alloys after a heat treatment may be complex. It may depend not only on the alloy composition but also on casting technology and thermo-mechanical treatment [4, 5]. A deeper understanding of the precipitation processes in such alloys is essential for the tailored design of alloys with properties required by specific applications. The remarkable interest in Mg-Y-Nd-based alloys as potential degradable materials for implants has led to numerous publications in this field, e. g. Refs. [1, 9, 10].

Calorimetric data in scanning conditions (DSC) have been proved to be a powerful tool in characterizing the structure evolution of supersaturated Mg alloys, giving also useful hints for design and modifications of thermal treatments [11-14].

In the present study, the calorimetric technique in scanning conditions has been adopted for the first time at our best knowledge on a Mg-Y-Nd alloy with Sc and Mn content. Aiming to investigate the phase transformations induced by thermal treatments, attention has been paid on a phenomenological description of the structural modifications and its relevance on the electrical resistivity and microhardness.

2. EXPERIMENTAL DETAILS

Magnesium Mg - 3.7 wt.% Y - 2.1 wt.% Nd - 1.3 wt.% Sc - 1.2 wt.% Mn alloy was squeeze cast under a protective gas atmosphere (Ar + 1 % SF_6). The composition of the alloy was very close to the composition of the alloy used in Refs. [4, 5].

Differential scanning calorimetry of the Mg-Y-Nd-Sc-Mn alloy was performed at heating rates of 0.5, 1, 2, 5, 10, 20 and 30 $K \cdot min^{-1}$ in the Netzsch DSC 200 F3 apparatus. The specimen of mass between 10-15 mg was placed in Al_2O_3 crucibles. Measurements were performed without a reference. Nitrogen flowed with the rate of 40 ml/min as a protective atmosphere.

The ranges of phase transformations in the alloy were also determined by electrical resistivity and hardness (HV3) measurements in the isochronal annealing mode in steps of 30 K/30 min. The heat treatment was carried out in a stirred oil bath up to 240 °C and in a furnace with Ar-protective atmosphere at higher temperatures. Each step was followed by quenching; resistivity was measured at 78 K after each annealing step and at room temperature (RT) in ethanol bath after heat treatment at selected temperatures. The influence of isochronal annealing on mechanical properties was studied using Vickers hardness measurements at RT following the same procedure as in resistivity measurements. The measurement started no longer than 5 minutes after the heat treatment step to minimise eventual natural ageing [15]. The H-shaped specimens were used for resistivity measurements. Relative electrical resistivity changes $\Delta\rho/\rho_0$ were obtained to within an accuracy of 10^{-4} (ρ_0 is the value of resistivity in the initial state). Resistivity was measured by the DC four-point method with a dummy specimen in series. The influence of parasitic thermo-electromotive force was suppressed by current reversal. The ratio *RRR* of the electrical resistivity at RT to that at 78 K: $RRR = \rho_{295\,K}/\rho_{78\,K}$ does not depend on the specimen shape and corresponds to a relative Mg-matrix purity.

Transmission electron microscopy (TEM) and electron diffraction (ED) were carried out in a JEOL JEM 2000FX electron microscope to determine the microstructure of the alloy. The specimens were prepared by the same isochronal annealing procedure as those for electrical resistivity and hardness measurements at heating rate of 1 K/min. The analysis of precipitated phases was supported by energy-dispersive X-ray spectroscopy performed by an X-ray BRUKER microanalyser.

3. RESULTS AND DISCUSSION

Density of the squeeze-cast Mg-Y-Nd-Sc-Mn alloy was determined as (1845 ± 10) kg/m^3. The density value was calculated as 1837 kg/m^3 for the simple mixture of elements not reflecting the real phase composition of the squeeze-cast alloy. However, it can be concluded that the alloy showed very little porosity. The alloy in the as-prepared state exhibited a microstructure with cellular grains of size ~ 70 μm.

Fig. 1 shows the response of the relative resistivity changes and hardness HV3 to step-by-step isochronal annealing in the alloy up to 510 °C. The electrical resistivity curve shows a slight decrease of $\Delta\rho/\rho_0$ followed by an increase up to 240 °C. The hardness increase is observed already at 90 °C. The main feature is the resistivity decrease with the minimum at ~ 360 °C. The main decrease in concentration of matrix scattering centres for conduction electrons can be expected up to this temperature. Almost no changes in the hardness connected to these processes were observed. The electrical resistivity increase in the temperature range of 390 - 510 °C indicates dissolution of some precipitated phases.

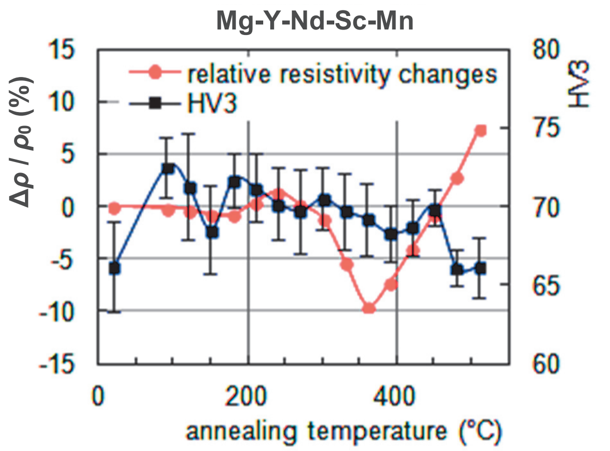

Fig. 1 Isochronal annealing curves of relative resistivity changes (measured at 78 K) and hardness HV3 changes with standard deviation. ρ_0 is the initial value of electrical resistivity, annealing was performed in 30 K/30 min steps

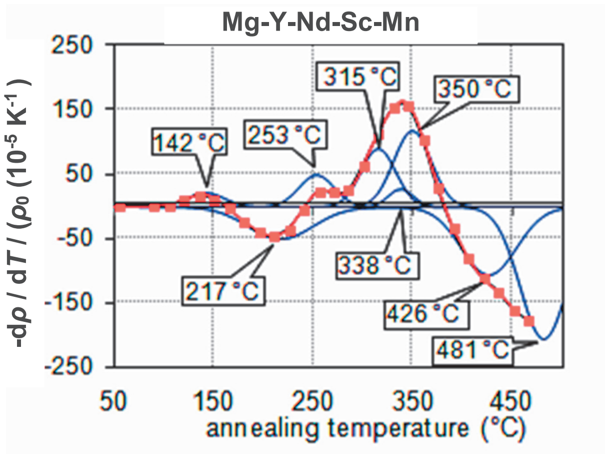

Fig. 2 Spectrum derived as derivative of the isochronal resistivity-annealing curve of the alloy fitted by Gaussian curves of single annealing stages. ρ_0 is the initial value of electrical resistivity

Negative numerical derivatives of the measured resistivity annealing curve from **Fig. 1** are plotted in **Fig. 2** for a better recognition. The obtained spectrum can be fitted by Gaussian curves using the method of least squares [4]. One can see the low stage with a maximum at 142 °C followed by one low negative stage at 217 °C and the more pronounced positive stage at 253 °C. The next distinctive positive stage is composed of three sub-stages at 315, 338 and 350 °C. The dissolution is composed of two negative stages at 426 °C, lower one, and at 481 °C, the pronounced one.

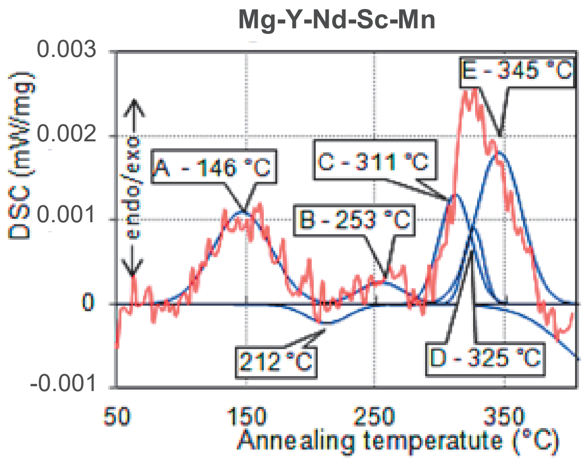

Fig. 3 DSC trace (red solid line) in linear heating program 1 K/min of the Mg-Y-Nd-Sc-Mn alloy fitted up to 405 °C by Gaussian curves (blue solid lines) of single thermal processes

Differential scanning calorimetry revealed three exothermic effects connected to precipitation processes. The temperature position of the heat effects shifts to higher temperatures with the increasing heating rate. For illustration, **Fig. 3** shows the DSC curve at heating rate of 1 K/1 min where up to five exothermic heat effects, marked A-E, can be distinguished by Gaussian curves. Weak thermal effects B, C and D were detected only for heating rates of 1 and 5 K/min. It is seen that exothermic effects are connected with negative resistivity changes and with positions of the resistivity spectra stages - compare **Figs. 1, 2** and **3** - the maxima of spectra from **Fig. 2** agree well with DSC results from **Fig. 3**.

The Kissinger method [16] with the assumption that the peak temperature T_m in DSC curves for individual precipitation effects can be expressed as

$$\ln(\Phi/T_m^2) = - Q / (R\, T_m) + C, \qquad (1)$$

where C is a constant, Q the precipitation process activation energy, R the gas constant, Φ the heating rate.

Table 1 Activation energies of the precipitation processes (effect A and effect E) in the Mg-Y-Nd-Sc-Mn alloy determined by the Kissinger method

Process	Effect A (β'' phase)	Effect E (β phase)
Activation energy	(119 ± 10) kJ/mol	(147 ± 10) kJ/mol

Fig. 4 shows the Kissinger plot in the coordinate system of [ln(Φ/T_m^2); $1/T_m$]. The apparent activation energy values obtained for the individual precipitation processes A and E from the slope of the Kissinger plot are listed in **Table 1**.

No evidence for a precipitation process was found by TEM and ED in the temperature range of the first stage in the alloy. As this early stage is already associated with a thermal effect A and with a small hardness increase, we suppose a submicroscopic spherical particle formation of a transient β'' phase with the $D0_{19}$ structure there. Furthermore, the observed activation energy, Q_A = (119 ± 10) kJ·mol^{-1}, corresponds well to the values obtained for precipitation of the β'' phase with $D0_{19}$ structure by calorimetry in the MgTbNd alloy [15] and squeeze-cast Mg3Y3Nd alloy [7]. It is probable that the following resistivity annealing negative stage at 217 °C and endothermic effect at 212 °C come from the dissolution of transient phase known from the Mg-Y-Nd system.

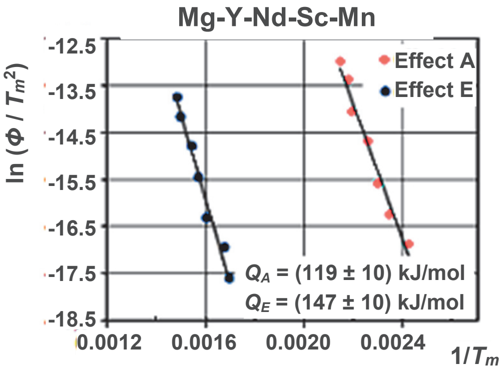

Fig. 4 Kissinger plot of exothermic heat effects (A - β'' phase with $D0_{19}$ structure, E - stable β-phase) in the squeeze-cast MgYNdScMn alloy. ϕ is the linear heating rate; T_m is the peak temperature of DSC trace for particular exothermic heat effect

The precipitation of transient β' phase with the c-base-centred orthorhombic (cbco) structure in the form of fine plates parallel to prismatic planes of the matrix was observed by TEM in the alloy after annealing up to 270 °C [4]. Precipitation of the same phase was also observed in the WE43 alloy [9,11,12]. Thus the resistivity stage at 253 °C comes from the precipitation of this transient phase. A weak thermal reaction labelled as B (see **Fig. 3**) corresponding to this process was not detected at all heating rates and activation energy of the process was therefore not calculated.

The separation of precipitation stages by resistivity measurements of the alloy in **Fig. 2** enables to determine individual processes above ~ 270 °C. The transient β' phase transforms into a stable β phase of the Mg_5Gd-type after subsequent annealing in the alloy. The equilibrium Mg-Y-Nd phase has the fcc structure and precipitates as plates parallel to prismatic planes. In addition, the Mn_2Sc incoherent phase in the form of fine discs parallel to the matrix basal planes was observed at the same annealing temperature (390 °C), simultaneously with very thin basal plates of a transient hexagonal phase containing rare earths and Mn. The same transient hexagonal phase was observed in other Mg-RE alloys with Sc and Mn [4, 5, 17]. The microstructure shown in **Fig. 5** documents the presence of all three phases. The analysis of the DSC trace and spectrum resistivity curve in heating rate 1 K/1 min confirmed that the main stage is also composed of all three stages and has its nature in the precipitation of the Mn_2Sc phase, precipitation of tiny hexagonal basal plates containing Y and Mn and the equilibrium β phase of the Mg-Y-Nd system. Values of the ratio *RRR* also reveal a decreasing concentration of solutes in the matrix on annealing up to the resistivity minimum in the alloy - see **Table 2**.

Table 2 RRR = ρ_{295K}/ρ_{78K} for the alloy in the squeeze-cast state, isochronally annealed up to 360 °C and annealed up to 510 °C

Annealing temperature (°C)	RT	360	510
RRR	1.443	1.1703	1.1338

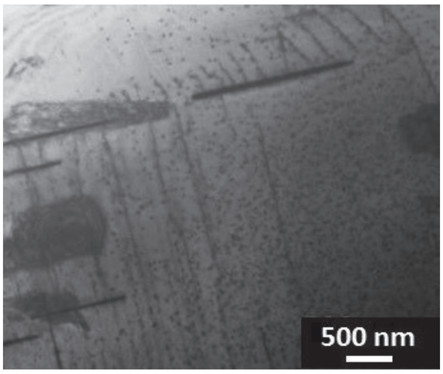

Fig. 5a TEM bright field image of the MgYNdScMn alloy isochronally annealed up to 390 °C. See fine Mn_2Sc basal disc and stable β phase prismatic plates

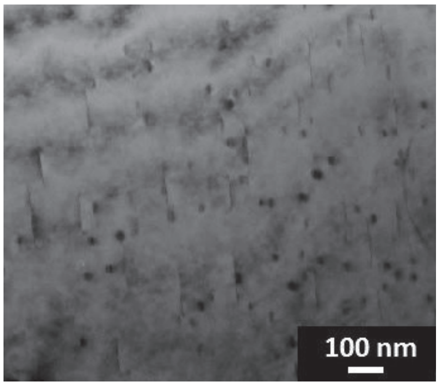

Fig. 5b TEM bright field image of the MgYNdScMn alloy isochronally annealed up to 390 °C. See fine Mn_2Sc basal disc and thin hexagonal basal plates

The distinct exothermic heat effect enabled to determine the activation energy for the stable β phase precipitation. The observed activation energy for the β phase formation, Q_E = (147±10) kJ/mol, corresponds well to the results obtained in Mg3Nd3Y alloy (Q = (147±10) kJ/mol [14]) and WE43 alloy (Q = (147±10) kJ/mol [14], Q = 177 kJ/mol [12]).

The electrical resistivity increase in the temperature range 390 - 510 °C indicates dissolution of some precipitated phases. The Mn_2Sc phase particles do not contribute to decrease of matrix purity as they do not dissolve and coarsen only to the size of 20 - 60 nm even by annealing up to 510 °C. No phases containing Y or Nd were detected by TEM after step-by-step annealing above 420 °C. The dissolution of some precipitated phases is confirmed by the existence of two negative resistivity stages at 426 °C, lower one, and 481 °C, the pronounced one, as well as endothermic thermal effect at temperatures higher 390 °C. It agrees also well with the evident decrease of the values of ratio *RRR* of the alloy isochronally annealed up to 510 °C (see **Table 2**) in comparison to the values of ratio *RRR* at 360 °C. The lower *RRR* value (see **Table 2**) at 510 °C confirms this conclusion.

CONCLUSIONS

Microstructure observation showed the formation of a submicroscopic particles of a transient β“ phase and the precipitation of the transient β‘ phase in the form of fine prismatic plates. The Mn_2Sc discs parallel to basal planes and thin basal Mn, Y-containing plates of a transient hexagonal phase were observed simultaneously with formation of the stable β phase. These processes overlapping in temperature range stabilize the hardness up to 450 °C. Only coarsening of the Mn_2Sc phase particles were found above 390 °C. The activation energies for precipitation of the $D0_{19}$ submicroscopic particles and precipitation of the stable β phase were calculated. The DSC results on phase precipitation in the Mg-Y-Nd-Sc-Mn correspond very well to the electrical resistivity response.

ACKNOWLEDGEMENTS

The work is a part of activities of the Charles University Research Centre "Physics of Condensed Matter and Functional Materials". Financial support in frame of the project GACR P108/10/0648 is also gratefully acknowledged.

REFERENCES

[1] HORT, N., HUANG, Y., FECHNER, D., STÖRMER, M., BLAWERT, C., WITTE, F., VOGT, C., DRÜCKER, H.,

WILLUMEIT, R., KAINER, K.U., FEYERABEND, F. Magnesium Alloys as Implant Materials - Principles of Property Design for Mg-RE alloys, *Acta Biomaterialia,* 2010, Vol. 6, Issue 5, pp. 1741-1725, doi.10.1016/j.actbio.2009.09.010.

[2] ISSA, A., SAAL, J.E., WOLVERTON, C. Physical Factors Controlling the Observed High-strength Precipitate Morphology in Mg-rare earth alloys, *Acta Materialia*, 2014, Vol. 65, pp. 240-250, doi.10.1016/j.actamat.2013.10.066.

[3] GRÖBNER, J., SCHMID-FETZER, R. Thermodynamic Modeling of the Mg-Ce-Gd-Y System, *Scripta Materialia,* 2010, Vol. 63, pp. 674-679, doi.10.1016/j.scriptamat.2010.01.035.

[4] STULÍKOVÁ, I., SMOLA, B. Identification and Characterization of Phase transformations by the Resistivity Measurements in Mg-RE-Mn Alloys, *Solid State Phenomena*, 2008, Vol. 138, pp. 57-62, doi.10.4028/www.scientific.net/SSP.138.57.

[5] STULÍKOVÁ, I., SMOLA, B., PELCOVÁ, J., VLACH, M., MORDIKE, B. L. Phase Transformations in Creep Resistant MgYNdScMn Alloy, *Z. Metallkd*., 2005, Vol. 96, Issue 7, pp. 821-825, doi.10.3139/146.101108.

[6] NIE, J.F., MUDDLE, B.C. Characterization of Strengthening Precipitate Phases in a Mg-Y-Nd Alloy*, Acta Materialia*, 2000, Vol. 48, Issue 8, pp. 1691-1703, doi.10.1016/S1359-6454(00)00013-6.

[7] GAO, Y., LIU, H., SHI, R., ZHOU, N., XU, Z., ZHU, Y.M., NIE, J.F., WANG, Y. Simulation Study of Precipitation in an Mg-Y-Nd Alloy*, Acta Materialia*, 2012, Vol. 60, Issue 12, pp. 4819-4832, doi.10.1016/j.actamat.2012.05.013.

[8] SMOLA, B., STULÍKOVÁ, I. Structure and Identification of Transient and Equilibrium Phases in Mg Alloys Containing Rare Earth Elements, *Metallic Materials*, 2004, Vol. 42, Issue 5, pp. 301-315.

[9] GU, X.N., ZHOU, Y.F., ZHENG, Y.F., CHENG, Y., WEI, S.C., ZHONG, S.P., XI, T.F., CHEN, L.J. Corrosion Fatigue Behaviours of Two Biomedical Mg Alloys - AZ91D and WE43 - In Simulated Body Fluid, *Acta Biomaterialia*, 2010, Vol. 6, pp. 4605-4613, doi.10.1016/j.actbio.2010.07.026.

[10] SMOLA, B., JOSKA, L., BŘEZINA, V., STULÍKOVÁ, I., HNILICA, F. Microstructure, Corrosion Resistance and Cytocompatibility of Mg-5Y-4Rare Earth-0.5Zr (WE54) Alloy, *Mater. Sci. Eng*., 2012, Vol. C 32, pp. 659-664, doi.10.1016/j.msec.2012.01.003.

[11] RIONTINO, G., LUSSANA, D., MASSAZZA, M., ZANADA, A. DSC Investigation on WE43 and Elektron 21 Mg Alloys, *J. Mater. Sci*., 2006, Vol. 41, pp. 3167-3169, doi.10.1007/s10853-006-6375-4.

[12] RIONTINO, G., LUSSANA, D., MASSAZZA, M. A Calorimetric Study of Phase Evolution in a WE43 Mg Alloy, *Journal of Thermal Analysis and Calorimetry*, 2006, Vol. 83, Issue 3, pp. 643-647, doi.10.1007/s10973-005-7125-6.

[13] SMOLA, B., STULÍKOVÁ, I., ČERNÁ, J., ČÍŽEK, J., VLACH, M. Phase Transformations in MgTbNd Alloy, *Physics Status Solidi A*, 2011, Vol. 1-8, doi.10.1002/pssa.201127296.

[14] VLACH, M., SMOLA, B., CÍSAŘOVÁ, H., STULÍKOVÁ, I. Precipitation Processes in Mg-Y-Nd alloys, *Defect Dif. Forum*, 2013, Vol. 334 - 335, pp. 155-160, doi: 10.4028/www.scientific.net/DDF.334-335.155.

[15] ČÍŽEK, J., SMOLA, B., STULÍKOVÁ, I., HRUŠKA, P., VLACH, M., VLČEK, M., MELIKHOVA, O., PROCHÁZKA, I. Natural Aging of Mg-Gd and Mg-Tb Alloys, *Physics Status Solidi*, 2012, Vol. 209, Issue 11, pp. 2135-2141, doi.10.1002/pssa.201228327.

[16] STARINK, M.J. The Determination of Activation Energy form Linear heating Rate Experiments: a Comparison of the Accuracy of Isoconversion Methods, *Thermochimica Acta*, 2003, Vol. 404, Issue 1-2, pp.163-176, doi.10.1016/S0040-6031(03)00144-8.

[17] SMOLA, B., STULÍKOVÁ, I., PELCOVÁ, J., von BUCH, F., MORDIKE, B. L. Phase Transformations due to Isochronal Annealing of Mg-rare earth-Sc-Mn Squeeze Cast Alloys, *Zeitschrift für Metallkunde*, 2003, Vol. 94, Issue 5, pp. 553-558, doi.10.3139/146.030553.